Structure formation constraints on the Jordan-Brans-Dicke theory

Viviana Acquaviva,[1,2,3] Carlo Baccigalupi,[1,2] Samuel M. Leach,[1,4] Andrew R. Liddle,[3] and Francesca Perrotta[1,2]

[1]*SISSA/ISAS, Via Beirut 4, 34014 Trieste, Italy*
[2]*INFN, Sezione di Trieste, Via Valerio 2, 34127 Trieste, Italy*
[3]*Astronomy Centre, University of Sussex, Brighton BN1 9QH, United Kingdom*
[4]*Département de Physique Théorique, Université de Genève, 24 quai Ernest Ansermet, CH-1211 Genève 4, Switzerland*

We use cosmic microwave background data from WMAP, ACBAR, VSA and CBI, and galaxy power spectrum data from 2dF, to constrain flat cosmologies based on the Jordan-Brans-Dicke theory, using a Markov chain Monte Carlo approach. Using a parametrization based on $\xi = 1/4\omega$, and performing an exploration in the range $\ln\xi \in [-9, 3]$, we obtain a 95% marginalized probability bound of $\ln\xi < -6.2$, corresponding to a 95% marginalized probability lower bound on the Brans-Dicke parameter $\omega > 120$.

I. INTRODUCTION

Jordan-Brans-Dicke (JBD) theory [1,2] is the simplest extended theory of gravity, depending on one additional parameter, the Brans-Dicke coupling ω, as compared to general relativity. As Einstein's theory is recovered in the limit $\omega \to \infty$, there will always be viable JBD theories as long as general relativity remains so too. As such, it acts as a laboratory for quantifying how accurately the predictions of general relativity stand up against observational tests. The most stringent limits are derived from radar timing experiments within our solar system, with measurements using the Cassini probe [3] now giving a two-sigma lower limit $\omega > 40\,000$ (improving preexisting limits [4] by an order of magnitude).

With precision cosmological data now available, particularly on cosmic microwave background (CMB) anisotropies from the Wilkinson Microwave Anisotropy Probe (WMAP) [5], it has become feasible to obtain complementary constraints from the effect of modified gravity on the structure formation process, as suggested in Ref. [6]. That paper focused on the way that ω alters the Hubble scale at matter-radiation equality, which is a scale imprinted on the matter power spectrum, in an attempt to identify how large an effect can be expected. Subsequently, the expected total intensity and polarization microwave anisotropy spectra in the JBD theory were computed, and a forecast of the sensitivity to ω of data from the WMAP and Planck satellites carried out exploiting a Fisher matrix approach [7].

In this paper we make a comprehensive comparison of predictions of the JBD theory to current observational data, using WMAP and other CMB data plus the galaxy power spectrum as measured by the two-degree field (2dF) galaxy redshift survey. We define JBD models in terms of eight parameters, which are allowed to vary simultaneously. Our paper is closest in spirit to work by Nagata *et al.* [8], who considered a more general model, the harmonic attractor model, which includes JBD as a special case. However

their data set compilation was restricted to the WMAP temperature power spectrum.

The constraint we will obtain is not competitive with the very stringent solar system bound given above (though the analysis of Ref. [7] indicates that a limit as high as 3000 might eventually be reached by the measurements of the Planck satellite), but it is complementary in that it applies on a completely different length and time scale. Such constraints can therefore still be of interest in general scalar-tensor theories where ω is allowed to vary; for instance Nagata *et al.* [8] find that in some parameter regimes of the harmonic attractor model the cosmological constraint is stronger than the solar system one. In that regard, our result is most comparable to cosmological constraints imposed on ω from nucleosynthesis, which give only a weak lower limit of $\omega > 32$ [9].

II. FORMALISM

A. Background cosmology

The Lagrangian for the JBD theory is

$$\mathcal{L} = \frac{m_{\text{Pl}}^2}{16\pi}\left(\Phi R - \frac{\omega}{\Phi}\partial_\mu\Phi\partial^\mu\Phi\right) + \mathcal{L}_{\text{matter}}, \quad (1)$$

where the Brans-Dicke coupling ω is a constant, and $\Phi(t)$ is the Brans-Dicke (BD) field whose present value must give the observed gravitational coupling. We have included factors of m_{Pl} to define Φ as dimensionless.

The equations for a spatially flat Friedmann universe are [1,2,10]

$$\left(\frac{\dot{a}}{a}\right)^2 + \frac{\dot{a}}{a}\frac{\dot{\Phi}}{\Phi} = \frac{\omega}{6}\left(\frac{\dot{\Phi}}{\Phi}\right)^2 + \frac{8\pi}{3m_{\text{Pl}}^2\Phi}\rho; \quad (2)$$

$$\ddot{\Phi} + 3\frac{\dot{a}}{a}\dot{\Phi} = \frac{8\pi}{(2\omega+3)m_{\text{Pl}}^2}(\rho - 3p), \quad (3)$$

where $a(t)$ is the cosmological scale factor, and ρ and p are the energy density and pressure summed over all types of material in the Universe.
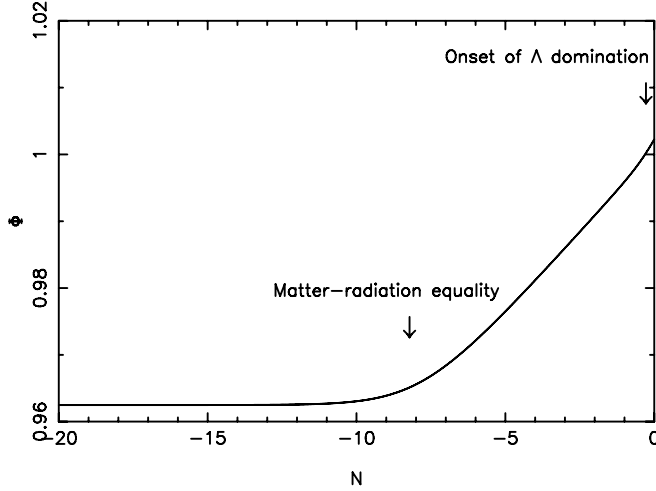
　　　　　　　　　　104025-1

FIG. 1. Evolution of the BD field from early in radiation domination to the present. It is just possible to see the evolution of Φ increase as Λ domination sets in. The cosmological parameters are $\omega = 200$, $H_0 = 72$, and $\rho_{m,0} = 0.3$ in units of the standard cosmology critical density.

The Universe is assumed to contain the same ingredients as the WMAP concordance model [5], namely, dark energy, dark matter, baryons, photons and neutrinos. We make the simplifying assumptions of spatial flatness, dark energy in the form of a pure cosmological constant, and effectively massless neutrinos whose density is related to that of photons by the usual thermal argument. The present value of Φ must correctly reproduce the strength of gravity seen in Cavendish-like experiments, which requires [2]

$$\Phi_0 = \frac{2\omega + 4}{2\omega + 3}, \qquad (4)$$

where here and throughout a subscript "0" indicates present value. We will assume that the value of Φ_0 in our solar system is representative of the Universe as a whole, though this may not be absolutely accurate [11]. We also assume that the initial perturbations are given by a power-law adiabatic perturbation spectrum.

When the Universe is dominated by a single fluid there are a variety of analytic solutions known [12], where Φ is typically constant during a radiation era, slowly increasing during a matter era, and then more swiftly evolving as dark energy domination sets in. However we need solutions spanning all three eras and so will solve the equations numerically, for which we use the integration variable $N \equiv \ln a/a_0$. An example of the evolution is shown in Fig. 1.

The basic parameter set we use to build our cosmological models contains the following parameters:

  ω Brans-Dicke coupling
  H_0 present Hubble parameter [$\mathrm{km\,s^{-1}\,Mpc^{-1}}$]
  ρ_B baryon density
  ρ_C cold dark matter density

  A_S curvature perturbation amplitude
  n_S perturbation spectral index
  τ reionization optical depth
  b galaxy bias parameter
where $b^2 = P_{gg}/P_{mm}$ is the ratio of the (observed) galaxy power spectrum to the (calculated) matter power spectrum. Other parameters are fixed by the assumptions above, and the radiation energy density is taken as fixed by the direct observation of the CMB temperature $T_0 = 2.725$ K [13].

An important subtlety that must be taken into account is that the extra terms in Eq. (2), plus the Cavendish-like correction to the present value of Φ, means that the usual relation between the Hubble parameter and density, used to define the critical density and hence density parameters, no longer applies. Generically, the extra terms require an increase in the present value of ρ to give the same expansion rate, the correction being of order $1/\omega$. Because of this subtlety, we define the density parameters $\Omega_{B,C}$ by dividing by the critical density for the standard cosmology, meaning that the density parameters do not quite sum to one for a spatially flat model.

Operationally, we proceed as follows. We seek a background evolution corresponding to a particular value of $h = H_0/100$ and of the present physical matter density. We can assume the initial velocity of the BD field $\dot{\Phi}$ is zero deep in the radiation era, which leaves us two parameters, the early time value of Φ and the value of the cosmological constant, to adjust in order to achieve the required values. This is a uniquely defined problem, with the necessary values readily found via an iterative shooting method.

B. Perturbation evolution

We carry out the evolution of density perturbations using a modified version of the code DEFAST, based on CMBFAST [14] and originally written to study quintessence scenarios where the dark energy scalar field is minimally [15] or nonminimally [16] coupled to the Ricci scalar. The architecture of DEFAST is based on the version 4.0 of CMBFAST, although there has been a progressive code fork in the subsequent versions. DEFAST takes as input the parameter set described in the previous subsection, and returns the microwave anisotropy spectra (for temperature and polarization) and the matter power spectrum. A dynamical and fluctuating scalar field, playing the role of the dark energy and/or the BD field, is included into the analysis together with the other cosmological components, following the existing general scheme [17].

In order to bring the model description into the formalism used by DEFAST, we redefine the BD field and coupling according to

$$\phi^2 = \omega \Phi \frac{m_{\mathrm{Pl}}^2}{2\pi}; \qquad \xi = \frac{1}{4\omega}, \qquad (5)$$

which brings the Lagrangian into the form

$$\mathcal{L} = \frac{1}{2}\xi\phi^2 R - \frac{1}{2}\partial_\mu\phi\partial^\mu\phi + \mathcal{L}_{\text{matter}}, \qquad (6)$$

where ϕ is now a canonical scalar field nonminimally coupled to gravity. We implement the cosmological constant in the code by giving ϕ a constant potential energy.

Our calculations include the effect of perturbations, with the initial perturbations in ϕ fixed by the requirement of adiabaticity. The correction to the background expansion rate from the dynamics of ϕ is the most relevant effect on the CMB power spectrum, appearing as a projection plus a correction to the integrated Sachs-Wolfe (ISW) effect, as discussed in detail in Ref. [16].

C. Data analysis

The data we use are taken from WMAP [18] and the 2dF galaxy redshift survey expressed as 32 bandpowers in the range $0.02 < k < 0.15h^{-1}$ Mpc [19]. In order to incorporate the 2dF data, the galaxy bias parameter b is taken to be a free parameter for which the analytic marginalization scheme of Ref. [20] can be applied. We also consider the effect of including the high-ℓ CMB data from the Very Small Array (VSA) [21], the Cosmic Background Imager (CBI) [22], and the Arcminute Cosmology Bolometer Array Receiver (ACBAR) [23].

Our present analysis does not include supernovae data. Inclusion of the modification to the luminosity distance from ω would be straightforward. However the variation of the gravitational coupling G means that supernovae can no longer be assumed to be standard candles, and Ref. [24] suggests that the effect from varying G dominates. Further, inclusion of supernovae data may be particularly susceptible to the possibility that the local value of Φ in the vicinity of the supernova may not match the global cosmological value [11]. Nevertheless, it would be interesting to investigate robust methods for including such data, also in connection with alternative observational strategies [25].

We carry out the data analysis using the now-standard Markov chain Monte Carlo (MCMC) posterior sampling technique, by modifying the June 2004 version of the COSMOMC program [26] to call DEFAST to obtain the spectra. COSMOMC computes the likelihood of the returned model and assembles a set of samples from the posterior distribution. We take full advantage of COSMOMC's parallel architecture by running the code across 19 Sun V60x Xeon 2.8GHz processors. The Metropolis-Hastings algorithm is run at a temperature of 1.3 in order to better sample the non-Gaussian direction of our posterior distribution which results from the degeneracy between H_0 and $\ln\xi$, both of which have a strong effect on the angular diameter distance. The final chains are then cooled and importance sampled [26]. It can be noted that for the purposes of posterior sampling, we have parametrized the JBD cosmology using $\ln\xi \equiv -\ln4\omega$ simply because it is more straightforward to obtain the samples we need, while si-

multaneously suppressing the possibility of jumping to regions with $\omega < 1$. Specifically, we use a flat prior on $\ln\xi \in [-9, -3]$ where the lower cutoff has been adjusted to the point where the likelihood function is no longer sensitive to the effect of varying the Brans-Dicke parameter and the ΛCDM model is thereby recovered. As usual, this Jeffreys prior, which is defined here as a flat prior on the logarithm of a parameter of unknown scale, has the interesting property of invariance under scale reparametrizations [27]. For this reason it serves as a reasonable substitute for working with a more desirable physical parameter which could be identified to isolate and give a linear response in the ISW effect, mainly responsible for the upper bound on $\ln\xi$.

The optical depth τ is parametrized using $Z = \exp[-2\tau]$, where $Z^{1/2}$ is the fraction of photons that remain unscattered through reionization, since the combination $A_S Z$ is well constrained by the CMB.

The results that we present are based on around 100 000 raw posterior samples, and while the basic constraints can be derived with significantly fewer samples, this large number assures more robust constraints on the derived parameter ω when we use importance sampling in order to adjust for the change in prior density [26].

III. OBSERVATIONAL CONSTRAINTS

Turning first to the constraints on the basic parameter set, from Fig. 2 we note the overall consistency of our results with the current observational picture (see, for example, Ref. [5] and a work by two of the current authors of Ref. [28]), finding the 99% marginalized probability regions to be
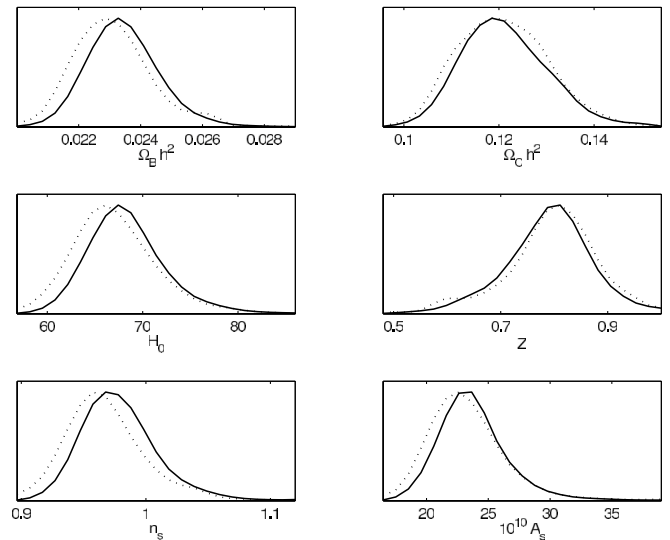

FIG. 2. Marginalized 1D posterior distributions (solid lines) on the base parameters as listed in Sec. II. Also displayed is the mean likelihood of the binned posterior samples (dotted lines).

$$0.021 < \Omega_B h^2 < 0.027, \qquad 0.10 < \Omega_C h^2 < 0.15,$$

$$61 < H_0 < 80, \qquad 0.57 < Z < 0.97, \qquad (7)$$

$$0.92 < n_S < 1.07, \qquad 19 < A_S < 33.$$

Note that part of our allowed region lies outside the priors assumed by Nagata *et al.* [8]. As usual for joint analyses of CMB and galaxy power spectrum data, it is unnecessary to impose a further constraint on H_0.

The primary focus of our study has been to derive constraints on the BD parameter for which, from the outset, we have expected only to find a one-sided bound; the situation can only become more interesting when both the angular diameter distance and the recombination history become much better probed by the CMB. This expectation is indeed confirmed by the data, as shown in Fig. 3 in which we display the region of highest posterior density. The lower panel detailing the posterior constraint on ω has been obtained by importance sampling to correct for the change in prior density when changing parameters from
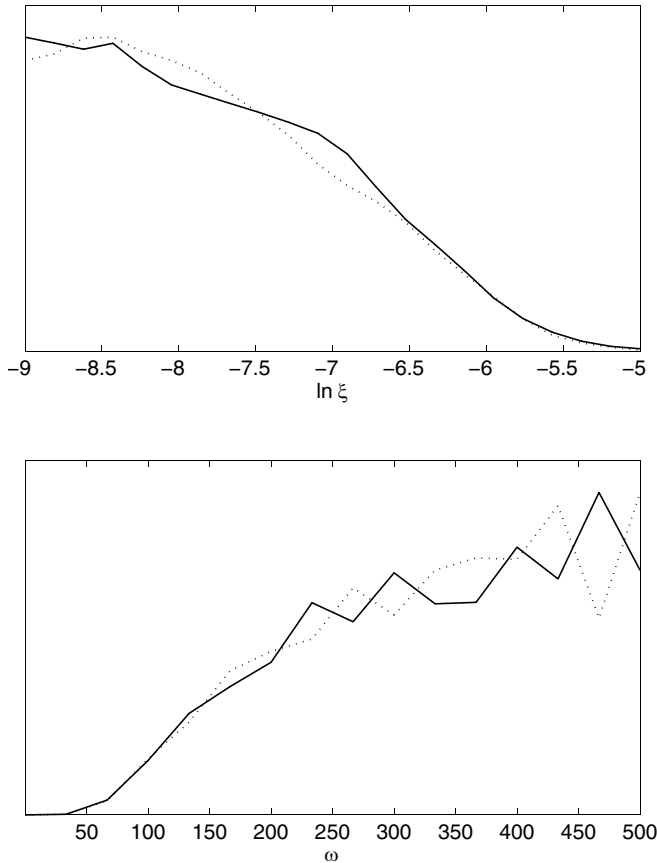

FIG. 3. Marginalized 1D posterior distributions (solid lines) on the BD parameter $\ln\xi$ (upper panel). Also displayed are the derived importance sampled constraints (correcting for the change in prior density) on the more familiar ω (lower panel, no smoothing). We obtain a 95% marginalized probability bound of $\ln\xi > -6.2$, corresponding to a bound on the BD parameter $\omega > 120$.

$\ln\xi$ to ω (we note that the mean likelihood of the binned posterior obtained from sampling $\ln\xi$ performs well for putting a bound on ω, demonstrating less sensitivity to the details of the prior density).

We calculate the marginalized probability upper bound and the main result of this paper to be

$$\ln\xi < -6.2, \quad 95\%, \qquad \ln\xi < -5.7, \quad 99\%. \quad (8)$$

The corresponding marginalized probability lower bounds on the BD parameter are found to be

$$\omega > 120, \quad 95\%, \qquad \omega > 80, \quad 99\%. \quad (9)$$

This bound is nicely consistent with the expectation for WMAP given by the Fisher matrix analysis of Ref. [7].

We present in Fig. 4 the 2D posterior constraints in the $\ln\xi$-H_0 plane, in order to demonstrate the degeneracy and covariance between these two parameters. In a more refined analysis, one could replace H_0 with the dimensionless parameter r_s/D_A more appropriate to the study of the CMB, where r_s is the sound horizon at recombination and D_A is the angular diameter distance to the last-scattering surface [29]. Finally, in Fig. 5 we display two models, our best-fit ΛCDM model with parameters $\theta \equiv \{\Omega_B h^2, \Omega_C h^2, H_0, Z, n_S, 10^{10}A_S, \omega\} = \{0.023, 0.12, 66, 0.79, 0.96, 23.2, \infty\}$, and a best-fit JBD model with parameters $\theta = \{0.024, 0.13, 79, 0.80, 1.03, 24, 70\}$, in order to illustrate how the observables change at finite ω. Here the JBD model lies in the vicinity the contour enclosing 99% of the posterior probability distribution and was selected by running a short Monte Carlo exploration at fixed $\omega = 70$. Note that although in principle the parameter $\ln\xi$ could be extended to $-\infty$, whereby the bulk of the parameter space would be composed of the ΛCDM model, in practice it is reasonable to adjust the lower cutoff to the point where the

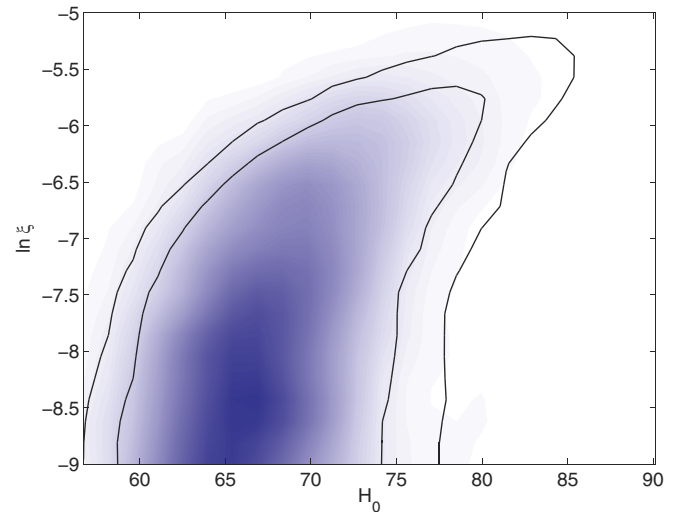

FIG. 4 (color online). Marginalized 2D posterior distribution in the $\ln\xi$-H_0 plane. The solid lines enclose 95% and 99% of the probability. Under this parametrization there is clearly a geometrical degeneracy.
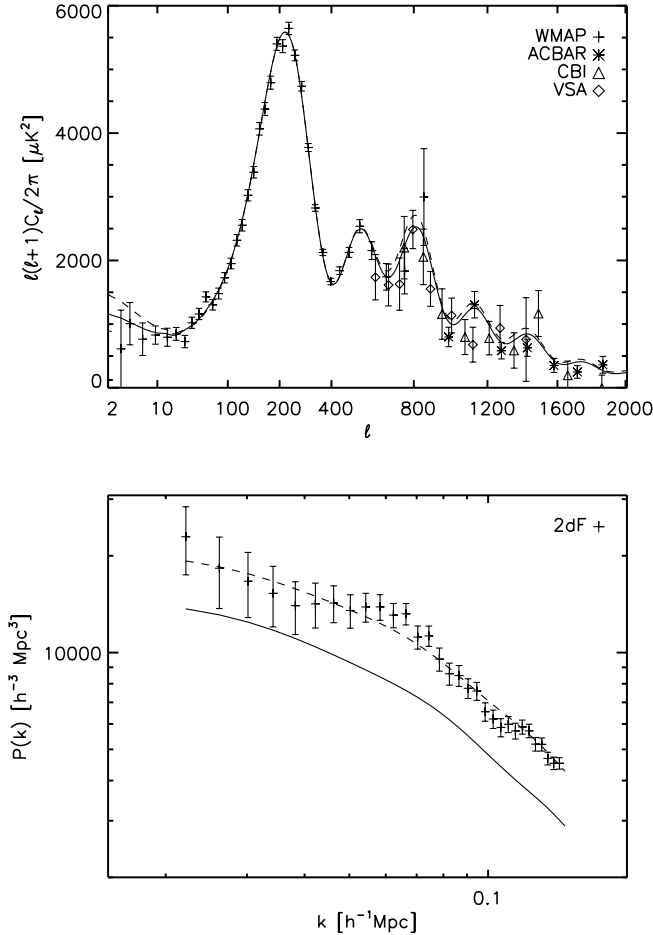
FIG. 5. A comparison between a ΛCDM model (solid line) and a JBD ΛCDM model with $\omega = 70$ (dashed line). The data are the 2dF galaxy power spectrum and the models the matter power spectrum convolved with the 2dF window functions, and whose overall amplitude is left as a free parameter. Detailed parameters are given in Sec. III.

likelihood function loses sensitivity to the variation of $\ln\xi$ so that the Brans-Dicke model alone is explored by the MCMC. Consequently, the probability contours can reasonably be interpreted to describe the most credible region of the Brans-Dicke model parameter space.

Our current analysis leaves the bias parameter free, and so constrains only the shape of the matter power spectrum. We note however that the JBD model has a significantly higher amplitude, indeed requiring a modest antibias $b \simeq 0.98$, which at least in part is due to the more rapid perturbation growth ($\delta \propto a^{1+1/\omega}$ during matter domination [6]) in the JBD theory. For comparison the ΛCDM model has a best-fit bias $b = 1.2$. This suggests that precision measures of the present-day matter spectrum amplitude, as for instance may become available via gravitational lensing, could significantly tighten constraints. We also note that there is a shift in the location of the baryon oscillations in the matter power spectrum as compared to the ΛCDM

model; these are mostly erased by the 2dF window function,[1] but future high-precision measurements of those may also assist in constraining ω.

We have carried out the same analysis including also the data from VSA, CBI and ACBAR in the multipole range $600 < \ell < 2000$. These high-ℓ data lead to a slightly tighter bound on the Brans-Dicke parameter, $\ln\xi < -6.4$ corresponding to $\omega > 177$ at 95% marginalized probability. However, at the same time inclusion of this new data leads to an unexpectedly large shift in the spectral index, to $0.90 < n_S < 1.00$ at 95% marginalized probability, so that the Harrison-Zel'dovich spectrum is only just included (this statement remains true in the general relativity limit). Whether this points to some emerging tension in the combined data set, a harmless statistical fluctuation, or a hint of the breaking of scale invariance, can be addressed only in the light of the next round of CMB observations. While our constraint on $\ln\xi$ marginalizes over n_S, in the interests of quoting a robust bound we have given as our main result the weaker limit obtained without including the high-ℓ data.

Our ultimate constraint $\omega > 120$ can be compared with that of Nagata *et al.* [8], who quote results corresponding to $\omega > 1000$ at two-sigma and $\omega > 50$ at four-sigma. The former constraint is much stronger than projected in Ref. [7], and stronger than one would expect from a naive assessment that the corrections to observables should be of order $1/\omega$. If we plotted a model with $\omega = 1000$ in our Fig. 5, it would lie practically on top of the ΛCDM model. However their latter constraint is in reasonable agreement with ours, and they do highlight that it is this constraint which corresponds to a sharp ridge of deteriorating chi-squared in their analysis, indicating that their constraint should conservatively be taken as $\omega > 50$.

IV. CONCLUSIONS

We have derived a constraint on Jordan-Brans-Dicke gravity from current cosmological observations, including CMB anisotropy data and the galaxy power spectrum data. Our main result is to obtain a 95% marginalized probability lower bound on the Brans-Dicke parameter $\omega > 120$. This result is complementary to the very strong solar system limit provided by Cassini, $\omega > 40\,000$, as it probes entirely different length and time scales. Our analysis is based on a Markov chain Monte Carlo technique varying the basic cosmological parameters and ω.

At the present precision level, the greatest part of the constraining power comes from the shape of the CMB acoustic peaks, in particular, from the first-year observations of WMAP. Therefore, assuming an extension to four

---

[1] Our analysis used 2dF data from Percival *et al.* [19], preceding the more recent 2dF data analysis which shows evidence of baryon oscillations [30]. We would not expect inclusion of this new data to significantly change our results.

years of the WMAP observations, we expect some further improvement on the limit on ω from cosmology. Further help is also expected from other structure formation data, as they improve quality and precision in coming years. In particular we have highlighted that an accurate measure of the present-day matter power spectrum amplitude, for instance from gravitational lensing, may be powerfully constraining when compared to the primordial amplitude from the CMB.

A leap forward in this and other contexts is expected from the observations of the Planck Surveyor probe, to be launched in 2007. Those observations are expected to be cosmic variance limited for the whole spectrum of CMB temperature anisotropy down to the damping tail, and to provide an accurate measurement of the gradient mode of the CMB polarization and its correlation with total intensity up to the sixth acoustic peak [31]. According to the forecasts of Chen and Kamionkowski [7], the limit on ω from Planck should be around an order of magnitude stronger than that from WMAP, and hence vastly stronger than the nucleosynthesis constraint. Whether that improvement can be realized from actual Planck data, of course, remains to be seen.

[1] C. Brans and R. H. Dicke, Phys. Rev. **124**, 925 (1961); P. J. E. Peebles and J. I. Yu, Astrophys. J. **162**, 815 (1970).

[2] C. M. Will, *Theory and Experiment in Gravitational Physics* (Cambridge University Press, Cambridge, 1993).

[3] B. Bertotti, L. Iess, and P. Tortora, Nature (London) **425**, 374 (2003).

[4] C. M. Will, Living Rev. Relativity **4**, 4 (2001), http://www.livingreviews.org/lrr-2001-4

[5] C. L. Bennett *et al.*, Astrophys. J. Suppl. Ser. **148**, 1 (2003); D. N. Spergel *et al.*, Astrophys. J. Suppl. Ser. **148**, 175 (2003).

[6] A. R. Liddle, A. Mazumdar, and J. D. Barrow, Phys. Rev. D **58**, 027302 (1998).

[7] X. Chen and M. Kamionkowski, Phys. Rev. D **60**, 104036 (1999).

[8] R. Nagata, T. Chiba, and N. Sugiyama, Phys. Rev. D **69**, 083512 (2004).

[9] T. Damour and B. Pichon, Phys. Rev. D **59**, 123502 (1999).

[10] S. Weinberg, *General Relativity and Cosmology* (Wiley, New York, 1972).

[11] T. Clifton, D. F. Mota, and J. D. Barrow, Mon. Not. R. Astron. Soc. **358**, 601 (2005).

[12] H. Nariai, Prog. Theor. Phys. **42**, 544 (1969); L. E. Gurevich, A. M. Finkelstein, and V. A. Ruban, Astrophys. Space Sci. **98**, 101 (1973).

[13] J. C. Mather *et al.*, Astrophys. J. **512**, 511 (1999).

[14] U. Seljak and M. Zaldarriaga, Astrophys. J. **469**, 437 (1996).

[15] F. Perrotta and C. Baccigalupi, Phys. Rev. D **59**, 123508 (1999).

[16] F. Perrotta, C. Baccigalupi, and S. Matarrese, Phys. Rev. D **61**, 023507 (2000); C. Baccigalupi, S. Matarrese, and F. Perrotta, Phys. Rev. D **62**, 123510 (2000).

[17] J. Hwang, Astrophys. J. **375**, 443 (1991).

[18] A. Kogut *et al.*, Astrophys. J. Suppl. Ser. **148**, 161 (2003); L. Verde *et al.*, Astrophys. J. Suppl. Ser. **148**, 195 (2003); G. Hinshaw *et al.*, Astrophys. J. Suppl. Ser. **148**, 135 (2003).

[19] W. J. Percival *et al.*, Mon. Not. R. Astron. Soc. **327**, 1297 (2001).

[20] S. L. Bridle *et al.*, Mon. Not. R. Astron. Soc. **335**, 1193 (2002).

[21] K. Grainge *et al.*, Mon. Not. R. Astron. Soc. **341**, L23 (2003); C. Dickinson *et al.*, astro-ph/0402498 [Mon. Not. R. Astron. Soc. (to be published)].

[22] T. J. Pearson *et al.*, Astrophys. J. **591**, 556 (2003); A. C. S. Readhead *et al.*, Astrophys. J. **609**, 498 (2004).

[23] C. L. Kuo *et al.*, Astrophys. J. **600**, 32 (2004).

[24] E. Gaztanaga, E. Garcia-berro, J. Isern, E. Bravo, and I. Dominguez, Phys. Rev. D **65**, 023506 (2002).

[25] B. Boisseau, G. Esposito-Farése, D. Polarski, and A. A. Starobinsky, Phys. Rev. Lett. **85**, 2236 (2000).

[26] A. Lewis and S. Bridle, Phys. Rev. D **66**, 103511 (2002).

[27] H. Jeffreys, *Theory of Probability* (Oxford University Press, Oxford, 1961), 3rd ed.

[28] S. M. Leach and A. R. Liddle, Phys. Rev. D **68**, 123508 (2003).

[29] A. Kosowsky, M. Milosavljevic, and R. Jimenez, Phys. Rev. D **66**, 063007 (2002); R. Jimenez, L. Verde, H. Peiris, and A. Kosowsky, Phys. Rev. D **70**, 023005 (2004).

[30] S. Cole *et al.*, astro-ph/0501174.

[31] S. Dodelson and W. Hu, Annu. Rev. Astron. Astrophys. **40**, 171 (2002).